Measurement of W-Boson Helicity Fractions in Top-Quark Decays Using $\cos\theta^*$

T. Aaltonen[14], J. Adelman[16], T. Akimoto[56], B. Álvarez González[27], S. Amerio[w30], D. Amidei[38], A. Anastassov[41], A. Annovi[35], J. Antos[13], G. Apollinari[18], A. Apresyan[49], T. Arisawa[58], A. Artikov[33], W. Ashmanskas[18], A. Attal[24], A. Aurisano[52], F. Azfar[44], P. Azzurri[z29], W. Badgett[18], A. Barbaro-Galtieri[17], V.E. Barnes[49], B.A. Barnett[53], V. Bartsch[12], G. Bauer[37], P.-H. Beauchemin[45], F. Bedeschi[29], D. Beecher[12], S. Behari[53], G. Bellettini[x29], J. Bellinger[60], D. Benjamin[15], A. Beretvas[18], J. Beringer[17], A. Bhatti[55], M. Binkley[18], D. Bisello[w30], I. Bizjak[cc12], R.E. Blair[1], C. Blocker[4], B. Blumenfeld[53], A. Bocci[15], A. Bodek[50], V. Boisvert[50], G. Bolla[49], D. Bortoletto[49], J. Boudreau[48], A. Boveia[8], B. Brau[a8], A. Bridgeman[23], L. Brigliadori[30], C. Bromberg[39], E. Brubaker[16], J. Budagov[33], H.S. Budd[50], S. Budd[23], S. Burke[18], K. Burkett[18], G. Busetto[w30], P. Bussey[k21], A. Buzatu[1], K. L. Byrum[1], S. Cabrera[u15], C. Calancha[11], M. Campanelli[39], M. Campbell[38], F. Canelli[18], A. Canepa[46], B. Carls[23], D. Carlsmith[60], R. Carosi[29], S. Carrillo[m19], S. Carron[45], B. Casal[27], M. Casarsa[18], A. Castro[v28], P. Catastini[y29], D. Cauz[bb32], V. Cavaliere[y29], M. Cavalli-Sforza[24], A. Cerri[17], L. Cerrito[n12], S.H. Chang[10], Y.C. Chen[47], M. Chertok[5], G. Chiarelli[29], G. Chlachidze[18], F. Chlebana[18], K. Cho[10], D. Chokheli[33], J.P. Chou[22], G. Choudalakis[37], S.H. Chuang[51], K. Chung[9], W.H. Chung[60], Y.S. Chung[50], T. Chwalek[25], C.I. Ciobanu[34], M.A. Ciocci[y29], A. Clark[20], D. Clark[4], G. Compostella[30], M.E. Convery[18], J. Conway[5], M. Cordelli[35], G. Cortiana[w30], C.A. Cox[5], D.J. Cox[5], F. Crescioli[x29], C. Cuenca Almenar[u5], J. Cuevas[r27], R. Culbertson[18], J.C. Cully[38], D. Dagenhart[18], M. Datta[18], T. Davies[21], P. de Barbaro[50], S. De Cecco[31], A. Deisher[17], G. De Lorenzo[24], M. Dell'Orso[x29], C. Deluca[24], L. Demortier[55], J. Deng[15], M. Deninno[28], P.F. Derwent[18], G.P. di Giovanni[34], C. Dionisi[aa31], B. Di Ruzza[bb32], J.R. Dittmann[3], M. D'Onofrio[24], S. Donati[x29], P. Dong[6], J. Donini[30], T. Dorigo[30], S. Dube[51], J. Efron[54], A. Elagin[52], R. Erbacher[5], D. Errede[23], S. Errede[23], R. Eusebi[18], H.C. Fang[17], S. Farrington[44], W.T. Fedorko[16], R.G. Feild[61], M. Feindt[25], J.P. Fernandez[11], C. Ferrazza[z29], R. Field[19], G. Flanagan[49], R. Forrest[5], M.J. Frank[3], M. Franklin[22], J.C. Freeman[18], I. Furic[19], M. Gallinaro[31], J. Galyardt[9], F. Garberson[8], J.E. Garcia[20], A.F. Garfinkel[49], K. Genser[18], H. Gerberich[23], D. Gerdes[38], A. Gessler[25], S. Giagu[aa31], V. Giakoumopoulou[2], P. Giannetti[29], K. Gibson[48], J.L. Gimmell[50], C.M. Ginsburg[18], N. Giokaris[2], M. Giordani[bb32], P. Giromini[35], M. Giunta[x29], G. Giurgiu[53], V. Glagolev[33], D. Glenzinski[18], M. Gold[40], N. Goldschmidt[19], A. Golossanov[18], G. Gomez[27], G. Gomez-Ceballos[37], M. Goncharov[52], O. González[11], I. Gorelov[40], A.T. Goshaw[15], K. Goulianos[55], A. Gresele[w30], S. Grinstein[22], C. Grosso-Pilcher[16], R.C. Group[18], U. Grundler[23], J. Guimaraes da Costa[22], Z. Gunay-Unalan[39], C. Haber[17], K. Hahn[37], S.R. Hahn[18], E. Halkiadakis[51],

Preprint submitted to Elsevier *November 5, 2008*

B.-Y. Han[50], J.Y. Han[50], F. Happacher[35], K. Hara[56], D. Hare[51], M. Hare[57], S. Harper[44], R.F. Harr[59], R.M. Harris[18], M. Hartz[48], K. Hatakeyama[55], C. Hays[44], M. Heck[25], A. Heijboer[46], J. Heinrich[46], C. Henderson[37], M. Herndon[60], J. Heuser[25], S. Hewamanage[3], D. Hidas[15], C.S. Hill[c8], D. Hirschbuehl[25], A. Hocker[18], S. Hou[47], M. Houlden[36], S.-C. Hsu[17], B.T. Huffman[44], R.E. Hughes[54], U. Husemann[61], M. Hussein[39], J. Huston[39], J. Incandela[8], G. Introzzi[29], M. Iori[aa31], A. Ivanov[5], E. James[18], B. Jayatilaka[15], E.J. Jeon[10], M.K. Jha[28], S. Jindariani[18], W. Johnson[5], M. Jones[49], K.K. Joo[10], S.Y. Jun[9], J.E. Jung[10], T.R. Junk[18], T. Kamon[52], D. Kar[19], P.E. Karchin[59], Y. Kato[43], R. Kephart[18], J. Keung[46], V. Khotilovich[52], B. Kilminster[18], D.H. Kim[10], H.S. Kim[10], H.W. Kim[10], J.E. Kim[10], M.J. Kim[35], S.B. Kim[10], S.H. Kim[56], Y.K. Kim[16], N. Kimura[56], L. Kirsch[4], S. Klimenko[19], B. Knuteson[37], B.R. Ko[15], K. Kondo[58], D.J. Kong[10], J. Konigsberg[19], A. Korytov[19], A.V. Kotwal[15], M. Kreps[25], J. Kroll[46], D. Krop[16], N. Krumnack[3], M. Kruse[15], V. Krutelyov[8], T. Kubo[56], T. Kuhr[25], N.P. Kulkarni[59], M. Kurata[56], S. Kwang[16], A.T. Laasanen[49], S. Lami[29], S. Lammel[18], M. Lancaster[12], R.L. Lander[5], K. Lannon[q54], A. Lath[51], G. Latino[y29], I. Lazzizzera[w30], T. LeCompte[1], E. Lee[52], H.S. Lee[16], S.W. Lee[t52], S. Leone[29], J.D. Lewis[18], C.-S. Lin[17], J. Linacre[44], M. Lindgren[18], E. Lipeles[46], A. Lister[5], D.O. Litvintsev[18], C. Liu[48], T. Liu[18], N.S. Lockyer[46], A. Loginov[61], M. Loreti[w30], L. Lovas[13], D. Lucchesi[w30], C. Luci[aa31], J. Lueck[25], P. Lujan[17], P. Lukens[18], G. Lungu[55], L. Lyons[44], J. Lys[17], R. Lysak[13], D. MacQueen[1], R. Madrak[18], K. Maeshima[18], K. Makhoul[37], T. Maki[14], P. Maksimovic[53], S. Malde[44], S. Malik[12], G. Manca[e36], A. Manousakis-Katsikakis[2], F. Margaroli[49], C. Marino[25], C.P. Marino[23], A. Martin[61], V. Martin[l21], M. Martínez[24], R. Martínez-Ballarín[11], T. Maruyama[56], P. Mastrandrea[31], T. Masubuchi[56], M. Mathis[53], M.E. Mattson[59], P. Mazzanti[28], K.S. McFarland[50], P. McIntyre[52], R. McNulty[j36], A. Mehta[36], P. Mehtala[14], A. Menzione[29], P. Merkel[49], C. Mesropian[55], T. Miao[18], N. Miladinovic[4], R. Miller[39], C. Mills[22], M. Milnik[25], A. Mitra[47], G. Mitselmakher[19], H. Miyake[56], S. Moed[22], N. Moggi[28], C.S. Moon[10], R. Moore[18], M.J. Morello[x29], J. Morlok[25], P. Movilla Fernandez[18], J. Mülmenstädt[17], A. Mukherjee[18], Th. Muller[25], R. Mumford[53], P. Murat[18], M. Mussini[v28], J. Nachtman[18], Y. Nagai[56], A. Nagano[56], J. Naganoma[56], K. Nakamura[56], I. Nakano[42], A. Napier[57], V. Necula[15], J. Nett[60], C. Neu[v46], M.S. Neubauer[23], S. Neubauer[25], J. Nielsen[g17], L. Nodulman[1], M. Norman[7], O. Norniella[23], E. Nurse[12], L. Oakes[44], S.H. Oh[15], Y.D. Oh[10], I. Oksuzian[19], T. Okusawa[43], R. Orava[14], S. Pagan Griso[w30], E. Palencia[18], V. Papadimitriou[18], A. Papaikonomou[25], A.A. Paramonov[16], B. Parks[54], S. Pashapour[45], J. Patrick[18], G. Pauletta[bb32], M. Paulini[9], C. Paus[37], T. Peiffer[25], D.E. Pellett[5], A. Penzo[32], T.J. Phillips[15], G. Piacentino[29], E. Pianori[46], L. Pinera[19], K. Pitts[23], C. Plager[6], L. Pondrom[60], O. Poukhov*[33],

*Deceased

N. Pounder[44], F. Prakoshyn[33], A. Pronko[18], J. Proudfoot[1], F. Ptohos[i 18], E. Pueschel[9], G. Punzi[x 29], J. Pursley[60], J. Rademacker[c 44], A. Rahaman[48], V. Ramakrishnan[60], N. Ranjan[49], I. Redondo[11], P. Renton[44], M. Renz[25], M. Rescigno[31], S. Richter[25], F. Rimondi[v 28], L. Ristori[29], A. Robson[21], T. Rodrigo[27], T. Rodriguez[46], E. Rogers[23], S. Rolli[57], R. Roser[18], M. Rossi[32], R. Rossin[8], P. Roy[1], A. Ruiz[27], J. Russ[9], V. Rusu[18], A. Safonov[52], W.K. Sakumoto[50], O. Saltó[24], L. Santi[bb 32], S. Sarkar[aa 31], L. Sartori[29], K. Sato[18], A. Savoy-Navarro[34], P. Schlabach[18], A. Schmidt[25], E.E. Schmidt[18], M.A. Schmidt[16], M.P. Schmidt[*61], M. Schmitt[41], T. Schwarz[5], L. Scodellaro[27], A. Scribano[y 29], F. Scuri[29], A. Sedov[49], S. Seidel[40], Y. Seiya[43], A. Semenov[33], L. Sexton-Kennedy[18], F. Sforza[29], A. Sfyrla[23], S.Z. Shalhout[59], T. Shears[36], P.F. Shepard[48], M. Shimojima[p 56], S. Shiraishi[16], M. Shochet[16], Y. Shon[60], I. Shreyber[26], A. Sidoti[29], P. Sinervo[45], A. Sisakyan[33], A.J. Slaughter[18], J. Slaunwhite[54], K. Sliwa[57], J.R. Smith[5], F.D. Snider[18], R. Snihur[1], A. Soha[5], S. Somalwar[51], V. Sorin[39], J. Spalding[18], T. Spreitzer[45], P. Squillacioti[y 29], M. Stanitzki[61], R. St. Denis[21], B. Stelzer[45], O. Stelzer-Chilton[1], D. Stentz[41], J. Strologas[40], G.L. Strycker[38], D. Stuart[8], J.S. Suh[10], A. Sukhanov[19], I. Suslov[33], T. Suzuki[56], A. Taffard[f 23], R. Takashima[42], Y. Takeuchi[56], R. Tanaka[42], M. Tecchio[38], P.K. Teng[47], K. Terashi[55], J. Thom[h 18], A.S. Thompson[21], G.A. Thompson[23], E. Thomson[46], P. Tipton[61], P. Ttito-Guzmán[11], S. Tkaczyk[18], D. Toback[52], S. Tokar[13], K. Tollefson[39], T. Tomura[56], D. Tonelli[18], S. Torre[35], D. Torretta[18], P. Totaro[bb 32], S. Tourneur[34], M. Trovato[29], S.-Y. Tsai[47], Y. Tu[46], N. Turini[y 29], F. Ukegawa[56], S. Vallecorsa[20], N. van Remortel[b 14], A. Varganov[38], E. Vataga[z 1], F. Vázquez[m 19], G. Velev[18], C. Vellidis[2], V. Veszpremi[49], M. Vidal[11], R. Vidal[18], I. Vila[27], R. Vilar[27], T. Vine[12], M. Vogel[40], I. Volobouev[t 17], G. Volpi[x 29], P. Wagner[46], R.G. Wagner[1], R.L. Wagner[18], W. Wagner[25], J. Wagner-Kuhr[25], T. Wakisaka[43], R. Wallny[6], S.M. Wang[47], A. Warburton[1], D. Waters[12], M. Weinberger[52], J. Weinelt[25], W.C. Wester III[18], B. Whitehouse[57], D. Whiteson[f 46], A.B. Wicklund[1], E. Wicklund[18], S. Wilbur[16], G. Williams[1], H.H. Williams[46], P. Wilson[18], B.L. Winer[54], P. Wittich[h 18], S. Wolbers[18], C. Wolfe[16], T. Wright[38], X. Wu[20], F. Würthwein[7], S.M. Wynne[36], S. Xie[37], A. Yagil[7], K. Yamamoto[43], J. Yamaoka[51], U.K. Yang[o 16], Y.C. Yang[10], W.M. Yao[17], G.P. Yeh[18], J. Yoh[18], K. Yorita[58], T. Yoshida[43], G.B. Yu[50], I. Yu[10], S.S. Yu[18], J.C. Yun[18], L. Zanello[aa 31], A. Zanetti[32], X. Zhang[23], Y. Zheng[d 6], and S. Zucchelli[v 28]

(CDF Collaboration[†])

[†]With visitors from [a]University of Massachusetts Amherst, Amherst, Massachusetts 01003, [b]Universiteit Antwerpen, B-2610 Antwerp, Belgium, [c]University of Bristol, Bristol BS8 1TL, United Kingdom, [d]Chinese Academy of Sciences, Beijing 100864, China, [e]Istituto Nazionale di Fisica Nucleare, Sezione di Cagliari, 09042 Monserrato (Cagliari), Italy, [f]University of California Irvine, Irvine, CA 92697, [g]University of California Santa Cruz, Santa Cruz, CA 95064, [h]Cornell University, Ithaca, NY 14853, [i]University of Cyprus, Nicosia CY-1678, Cyprus, [j]University College Dublin, Dublin 4, Ireland, [k]Royal Society of Edinburgh/Scottish Executive Support Research Fellow, [l]University of Edinburgh, Edinburgh EH9 3JZ, United King-

[1]Argonne National Laboratory, Argonne, Illinois 60439
[2]University of Athens, 157 71 Athens, Greece
[3]Baylor University, Waco, Texas 76798
[4]Brandeis University, Waltham, Massachusetts 02254
[5]University of California, Davis, Davis, California 95616
[6]University of California, Los Angeles, Los Angeles, California 90024
[7]University of California, San Diego, La Jolla, California 92093
[8]University of California, Santa Barbara, Santa Barbara, California 93106
[9]Carnegie Mellon University, Pittsburgh, PA 15213
[10]Center for High Energy Physics: Kyungpook National University, Daegu 702-701, Korea; Seoul National University, Seoul 151-742, Korea; Sungkyunkwan University, Suwon 440-746, Korea; Korea Institute of Science and Technology Information, Daejeon, 305-806, Korea; Chonnam National University, Gwangju, 500-757, Korea
[11]Centro de Investigaciones Energeticas Medioambientales y Tecnologicas, E-28040 Madrid, Spain
[12]University College London, London WC1E 6BT, United Kingdom
[13]Comenius University, 842 48 Bratislava, Slovakia; Institute of Experimental Physics, 040 01 Kosice, Slovakia
[14]Division of High Energy Physics, Department of Physics, University of Helsinki and Helsinki Institute of Physics, FIN-00014, Helsinki, Finland
[15]Duke University, Durham, North Carolina 27708
[16]Enrico Fermi Institute, University of Chicago, Chicago, Illinois 60637
[17]Ernest Orlando Lawrence Berkeley National Laboratory, Berkeley, California 94720
[18]Fermi National Accelerator Laboratory, Batavia, Illinois 60510
[19]University of Florida, Gainesville, Florida 32611
[20]University of Geneva, CH-1211 Geneva 4, Switzerland
[21]Glasgow University, Glasgow G12 8QQ, United Kingdom
[22]Harvard University, Cambridge, Massachusetts 02138
[23]University of Illinois, Urbana, Illinois 61801
[24]Institut de Fisica d'Altes Energies, Universitat Autonoma de Barcelona, E-08193, Bellaterra (Barcelona), Spain
[25]Institut für Experimentelle Kernphysik, Universität Karlsruhe, 76128 Karlsruhe, Germany
[26]Institution for Theoretical and Experimental Physics, ITEP, Moscow 117259, Russia
[27]Instituto de Fisica de Cantabria, CSIC-University of Cantabria, 39005 Santander, Spain
[28]Istituto Nazionale di Fisica Nucleare Bologna, [v]University of Bologna, I-40127 Bologna, Italy
[29]Istituto Nazionale di Fisica Nucleare Pisa, [x]University of Pisa, [y]University of Siena and [z]Scuola Normale Superiore, I-56127 Pisa, Italy
[30]Istituto Nazionale di Fisica Nucleare, Sezione di Padova-Trento, [w]University of Padova, I-35131 Padova, Italy
[31]Istituto Nazionale di Fisica Nucleare, Sezione di Roma 1, [aa]Sapienza Università di Roma, I-00185 Roma, Italy
[32]Istituto Nazionale di Fisica Nucleare Trieste/Udine, [bb]University of Trieste/Udine, Italy
[33]Joint Institute for Nuclear Research, RU-141980 Dubna, Russia
[34]LPNHE, Universite Pierre et Marie Curie/IN2P3-CNRS, UMR7585, Paris, F-75252 France
[35]Laboratori Nazionali di Frascati, Istituto Nazionale di Fisica Nucleare, I-00044 Frascati, Italy

dom, [m]Universidad Iberoamericana, Mexico D.F., Mexico, [n]Queen Mary, University of London, London, E1 4NS, England, [o]University of Manchester, Manchester M13 9PL, England, [p]Nagasaki Institute of Applied Science, Nagasaki, Japan, [q]University of Notre Dame, Notre Dame, IN 46556, [r]University de Oviedo, E-33007 Oviedo, Spain, [s]Texas Tech University, Lubbock, TX 79409, [t]IFIC(CSIC-Universitat de Valencia), 46071 Valencia, Spain, [u]University of Virginia, Charlottesville, VA 22904, [cc]On leave from J. Stefan Institute, Ljubljana, Slovenia

[36] University of Liverpool, Liverpool L69 7ZE, United Kingdom
[37] Massachusetts Institute of Technology, Cambridge, Massachusetts 02139
[38] University of Michigan, Ann Arbor, Michigan 48109
[39] Michigan State University, East Lansing, Michigan 48824
[40] University of New Mexico, Albuquerque, New Mexico 87131
[41] Northwestern University, Evanston, Illinois 60208
[42] Okayama University, Okayama 700-8530, Japan
[43] Osaka City University, Osaka 588, Japan
[44] University of Oxford, Oxford OX1 3RH, United Kingdom
[45] Institute of Particle Physics: McGill University, Montréal, Québec, Canada H3A 2T8; Simon Fraser University, Burnaby, British Columbia, Canada V5A 1S6; University of Toronto, Toronto, Ontario, Canada M5S 1A7; and TRIUMF, Vancouver, British Columbia, Canada V6T 2A3
[46] University of Pennsylvania, Philadelphia, Pennsylvania 19104
[47] Institute of Physics, Academia Sinica, Taipei, Taiwan 11529, Republic of China
[48] University of Pittsburgh, Pittsburgh, Pennsylvania 15260
[49] Purdue University, West Lafayette, Indiana 47907
[50] University of Rochester, Rochester, New York 14627
[51] Rutgers University, Piscataway, New Jersey 08855
[52] Texas A&M University, College Station, Texas 77843
[53] The Johns Hopkins University, Baltimore, Maryland 21218
[54] The Ohio State University, Columbus, Ohio 43210
[55] The Rockefeller University, New York, New York 10021
[56] University of Tsukuba, Tsukuba, Ibaraki 305, Japan
[57] Tufts University, Medford, Massachusetts 02155
[58] Waseda University, Tokyo 169, Japan
[59] Wayne State University, Detroit, Michigan 48201
[60] University of Wisconsin, Madison, Wisconsin 53706
[61] Yale University, New Haven, Connecticut 06520

Abstract

Fully reconstructed $t\bar{t} \to W^+bW^-\bar{b} \to \ell\nu q\bar{q}'b\bar{b}$ events are used to determine the fractions of right-handed (f_+) and longitudinally polarized (f_0) W bosons produced in top-quark decays. The helicity fractions are sensitive to the couplings and the Dirac structure of the Wtb vertex. This paper reports measurements of the W-boson helicity fractions from two different methods using data corresponding to an integrated luminosity of $1.9\,\mathrm{fb}^{-1}$ of $p\bar{p}$ collisions collected by the CDF II detector operating at the Fermilab Tevatron. Combining the results from the two methods, we find $f_0 = 0.62 \pm 0.10\,(\mathrm{stat}) \pm 0.05\,(\mathrm{syst})$ under the assumption that $f_+ = 0$, and $f_+ = -0.04 \pm 0.04\,(\mathrm{stat}) \pm 0.03\,(\mathrm{syst})$ with f_0 fixed to the theoretically expected value of 0.70. Model-independent fits are also performed and simultaneously determine $f_0 = 0.66 \pm 0.16\,(\mathrm{stat}) \pm 0.05\,(\mathrm{syst})$ and $f_+ = -0.03 \pm 0.06\,(\mathrm{stat}) \pm 0.03\,(\mathrm{syst})$. All these results are consistent with standard model expectations.

Key words: helicity, W boson, top quark
PACS: 12.15.-y, 13.38.Be, 13.88.+e, 14.65.Ha, 14.70Fm

1. Introduction

Charged current weak interactions proceed via the exchange of a $W^{\pm}$ boson and are theoretically described by a vertex factor that has a pure vector minus axial-vector ($V-A$) structure [1]. While weak interactions have been tested with high precision at low momentum transfers, e.g. in radioactive β-decay, the vertex structure may be altered in interactions at high momentum transfers due to new physics contributions. Among the known fundamental particles, the top quark stands out as the heaviest, with a mass of $m_t = 172.4 \pm 1.2$ GeV/c^2 [2], and thereby gives access to high momentum scales. It has been suggested that the top quark may have non-universal gauge couplings as a result of dynamical breaking of the electroweak symmetry [3].

Given our present knowledge of the Cabibbo-Kobayashi-Maskawa quark-mixing matrix [4], the top quark decays with a branching ratio close to 100% in the mode $t \to bW^+$. The Dirac structure of the Wtb vertex can be generalized by the interaction Lagrangian

$$\mathcal{L} = \frac{g_w}{\sqrt{2}} \left[W_\mu^- \bar{b} \gamma^\mu (f_1^L P_- + f_1^R P_+) t - \frac{1}{m_W} \partial_\nu W_\mu^- \bar{b} \sigma^{\mu\nu} (f_2^L P_- + f_2^R P_+) t \right] + h.c. \,, \tag{1}$$

where $P_\pm = \frac{1}{2}(1 \pm \gamma^5)$ and $i\sigma^{\mu\nu} = -\frac{1}{2}[\gamma^\mu, \gamma^\nu]$ [5]. In general the interaction of fermions and gauge bosons can be expressed by six form factors. Assuming the W boson to be on-shell, the number of form factors is reduced to four. These four form factors $f_{1,2}^{L,R}$ can assume complex values in general, but take values of $f_1^L = 1$ and $f_1^R = f_2^L = f_2^R = 0$ in standard electroweak theory, such that the production of right-handed W bosons from top-quark decay is suppressed. A general strategy to experimentally determine all four form factors in Eq. 1 involves the measurement of the W-boson helicity fractions and the measurement of the single top-quark production cross-section in the t-channel and in the s-channel [6].

The production of longitudinally polarized W bosons is enhanced due to the large Yukawa coupling of the top quark to the Higgs field responsible for electroweak symmetry breaking (EWSB). The fraction of right-handed W bosons, f_+, is predicted to be very small $\mathcal{O}(10^{-4})$ [7], which is well below the sensitivity of the measurements reported here. The partial decay widths into the different W-boson helicity states explicitly depend on the form factors. Assuming the standard electroweak theory values for the form factors the fraction of longitudinally polarized W bosons is given by $f_0 = \frac{\Gamma(W_0)}{\Gamma(W_0)+\Gamma(W_-)+\Gamma(W_+)} \approx \frac{m_t^2}{2m_W^2+m_t^2}$ [5] at leading order in perturbation theory, where W_0 and $W_\pm$ indicate longitudinally and transversely polarized W bosons, respectively. For m_t as given above and a W-boson mass of $m_W = 80.403 \pm 0.029$ GeV/c^2 [4] the theory predicts $f_0 = 0.697 \pm 0.002$. Next-to-leading-order corrections decrease the total decay width, as well as $\Gamma(W_0)$, by about 10% [8], while f_0 is only changed by about 1% [9]. A significant deviation of f_0 or f_+ from the predictions exceeding the 1% level would be a clear indication of new physics.

This article reports the results of two analyses using the same dataset and their combination. Both analyses use the observable $\cos\theta^*$, which is the cosine of the decay angle of the charged lepton in the W-boson decay frame measured with respect to the top-quark direction. This has the following distribution:

$$\omega(\theta^*) = f_0 \cdot \omega_0(\theta^*) + f_+ \cdot \omega_+(\theta^*) + (1 - f_0 - f_+) \cdot \omega_-(\theta^*) \quad \text{with} \quad (2)$$

$$\omega_0(\theta^*) = \frac{3}{4}(1 - \cos^2\theta^*), \omega_+(\theta^*) = \frac{3}{8}(1 + \cos\theta^*)^2, \omega_-(\theta^*) = \frac{3}{8}(1 - \cos\theta^*)^2. \quad (3)$$

The parameters f_0 and f_+ are the W-boson helicity fractions to be determined.

The two analyses estimate $\cos\theta^*$ for each event by reconstructing the full $t\bar{t}$ kinematics. These methods of reconstructing the four-vectors of the top-quark and antitop-quark as well as their decay products [10, 11, 12] possess a broad applicability and offer the possibility to measure a full set of top-quark properties, such as the top-quark mass and the forward-backward charge asymmetry in $t\bar{t}$ production [13]. Experimental acceptances and resolutions introduce distortions of the $\cos\theta^*$ distribution which must also be taken into account. The two analyses employ alternative methods for reconstructing the $t\bar{t}$ kinematics, for correcting the experimental effects, and for determining the polarization fractions from the resulting $\cos\theta^*$ distributions in the observed events. They have similar sensitivities and are combined, taking into account correlations, to yield the most precise estimates of f_0 and f_+. Both analyses subject the observed data to fits in three different scenarios:

1. Measure f_0 under the assumption that $f_+ = 0$. This corresponds to a model in which the form factors f_1^R and f_2^L are zero.
2. Measure f_+ under the assumption that $f_0 = 0.7$, which is sensitive to models with $f_2^L = f_2^R = 0$. Using the relation $f_+/f_- = (f_1^R/f_1^L)^2$ one can translate the measured helicity fractions into the ratio of form factors.
3. Measure f_0 and f_+ simultaneously in a two-parameter fit, which is model-independent.

Model-dependent measurements of f_0 and f_+ using smaller datasets have been previously reported by the CDF [14] and DØ [15] collaborations. Most recently the DØ collaboration has reported a model-independent result using 1 fb^{-1} [15] of Tevatron data. The measurements reported here use twice as much data and improved analysis techniques and yield the most precise determinations of the W-boson helicity fractions in top-quark decays.

2. The CDF II Detector

The data used for the analyses reported here are collected by the CDF II detector [16] which consists of a charged particle tracking system (including the central outer tracker, COT, which is an open-cell drift chamber, and a seven-layer silicon tracking system) enclosed within a magnetic field of 1.4 T, segmented electromagnetic and hadronic calorimeters, and muon detectors. The silicon microstrip detector provides tracking over the radial range 1.5-28 cm,

and is used to detect displaced secondary vertices. In the CDF geometry, θ is the polar angle with respect to the proton beam axis, and ϕ is the azimuthal angle. The pseudorapidity is $\eta \equiv -\ln(\tan(\theta/2))$. Detector $|\eta|$ is defined as the pseudorapidity of the jet calculated with respect to the center of the detector. The transverse momentum $p_{\rm T}$ is the component of the momentum projected onto the plane perpendicular to the beam axis. The transverse energy $E_{\rm T}$ of a shower or calorimeter tower is $E\sin\theta$, where E is the energy deposited. The missing $E_{\rm T}$ ($\vec{\not\!\!E}_{\rm T}$) is defined by $\vec{\not\!\!E}_{\rm T} = -\Sigma_i E^i_{\rm T}\mathbf{n}_i$, where $\mathbf{n}_i$ is the unit vector in the azimuthal plane that points from the beamline to the $i^{\rm th}$ calorimeter tower. We also define $\not\!\!E_{\rm T} = |\vec{\not\!\!E}_{\rm T}|$. The fiducial region of the silicon detector covers the pseudorapidity range $|\eta| < 2$, while the central tracking system and muon chambers provide coverage for $|\eta| < 1.5$. For electron identification we use the calorimeter region $|\eta| < 1$, while for jet identification we use $|\eta| < 2.5$. A three-level trigger system selects events with electron (muon) candidates with $E_{\rm T}$ ($P_{\rm T}$) > 18 GeV (18 GeV/c), which form the dataset for these analyses.

3. Selection of $t\bar{t}$ candidate events

We select events of the type $t\bar{t} \rightarrow W^+bW^-\bar{b} \rightarrow \ell\nu q\bar{q}'b\bar{b}$, which yield an experimental signature of one high energy charged lepton, missing transverse energy due to the undetected neutrino, and at least four jets, two of which are b-quark jets. Electrons are reconstructed as a track matched to an energy cluster in the central electromagnetic calorimeter. Muons are reconstructed as a COT track matched to a track segment in one of the muon chambers. Exactly one isolated electron candidate with $E_{\rm T} > 20$ GeV and $|\eta| < 1.1$ is required, or exactly one isolated muon candidate with $P_{\rm T} > 20$ GeV/c and $|\eta| < 1.0$. An electron or muon candidate is considered isolated if the $E_{\rm T}$ not assigned to the lepton in a cone of $R \equiv \sqrt{(\Delta\eta)^2 + (\Delta\phi)^2} = 0.4$, centered around the lepton, is less than 10% of the lepton $E_{\rm T}$ or $P_{\rm T}$, respectively. Jets are reconstructed by summing calorimeter energy in a cone of radius $R = 0.4$. The energy of the jets is corrected for differences as a function of η, time, and additional energy depositions due to multiple interactions occurring in the same event [17]. An additional correction leads from calorimeter based jets to jets at the particle level. Candidate jets must have corrected $E_{\rm T} > 20$ GeV and detector $|\eta| < 2$. Events are required to have at least four jets. The corrected $\not\!\!E_{\rm T}$ accounts for the energy corrections made for all jets with corrected $E_{\rm T} > 12$ GeV and $|\eta| < 2.4$ and for muons and is required to be greater than 20 GeV. At least one jet in the event has to contain a secondary vertex identified using the algorithm described in [18] and consistent with having originated from a b-hadron decay. Additional requirements further reduce the background contribution as follows. Electron events are rejected if the electrons originate from a conversion of a photon. Cosmic ray muon events are rejected as well. To remove Z bosons, events in which the charged lepton can be paired with any more loosely defined jet or lepton to form an invariant mass consistent with the Z peak, $76 - 106$ GeV/c^2, are excluded. With these selection criteria, we select 484 $t\bar{t}$ candidates in a

sample corresponding to a total integrated luminosity of 1.9 fb^{-1}.

Kinematic resolutions and selection and reconstruction efficiencies for $t\bar{t}$ events are determined utilizing PYTHIA [19] and HERWIG [20] event generators where the top-quark mass is set to 175 GeV/c^2. Samples of events generated with PYTHIA, ALPGEN [21], and MADEVENT [22], interfaced to PYTHIA parton showering are used to determine certain background rates and to estimate the $\cos\theta^*$ distribution for background events. In order to develop and validate the methods presented, MADEVENT and a custom version of HERWIG are used to generate samples of simulated events with controllable W-boson helicity fractions. All generated events are passed through the CDF detector simulation [23] and then reconstructed in the same way as the observed events.

4. Background Estimation

The selected $t\bar{t}$ sample is estimated to be contaminated with about 87 events coming from background processes. These non-$t\bar{t}$ processes originate mainly from W+jets events with a falsely reconstructed secondary vertex (Mistags), from W+jets events in which the jets are real b- and c-quark jets (W+heavy flavor), and multi-jet processes that contain no real W boson (non-W). These backgrounds are estimated using a combination of data and Monte Carlo methods as described in detail in [18]. Additional sources of background arise from electroweak processes like diboson production (WW, WZ, ZZ), the production of single top-quarks, and Z bosons. These backgrounds are predicted based on their theoretical cross sections and acceptances and efficiencies, which are derived from simulated events. Table 1 shows the background estimation and the observed number of events after all selection criteria.

Background source	N($\geq$ 4 jet)
W+heavy flavor	37 ± 10
Mistags	20 ± 5
non-W	18 ± 16
Electroweak	12 ± 1
Total background	87 ± 23
Observed events	484

Table 1: Expected number of background events and the number of observed events in a 1.9 fb^{-1} data sample using the selection criteria described in the text.

5. Extraction of the W-boson helicity fractions

In order to measure the W-boson helicity fractions we follow two approaches. Both analyses use $\cos\theta^*$ as the sensitive observable, estimated on an event-by-event basis by fully reconstructing the $t\bar{t}$ kinematics. The $\cos\theta^*$ distribution can be decomposed into three separate components according to the three different

W-boson helicity states. The first analysis is based on the methods developed to precisely measure the top-quark mass [10] and uses the fact that the three helicity components have distinguishable shapes. In this technique we find the expected distributions ("templates") of the helicity components, containing resolution effects, and superpose those. The helicity fractions are then given by normalizations from an unbinned likelihood fit and the results are corrected for acceptance effects afterwards [24]. We refer to this analysis as the "template analysis" in the following. The second analysis, called the "convolution analysis", is based on the method described in [14, 11, 12]. Starting from the theoretically predicted number of events in each bin of the particle level $\cos\theta^*$ distribution we convolute acceptance and resolution effects with these predictions to derive the expected number of events in each bin of the reconstructed $\cos\theta^*$ distribution. In this method, f_0 and f_+ are then determined from a binned likelihood fit.

The event selection and reconstruction of the two techniques employ different choices in the design of background suppression, jet flavor identification, and parton assignment. The agreement between the two methods shows that these design choices do not bias the final result. While the convolution analysis uses the standard event selection described in sec. 3, the template analysis chooses to place an additional cut on the scalar sum of all transverse energies of the event, H_{T}, and requires $H_{\mathrm{T}} > 250$ GeV to further suppress multi-jet non-W background. This results in 53 ± 20 events estimated as background, and reduces the total number of selected events to 430. A combinatoric ambiguity arises in the reconstruction of the $t\bar{t}$ kinematics when choosing which of the reconstructed jets corresponds to which of the final state quarks in the $t\bar{t} \to \ell\nu qq'b\bar{b}$ decay. The analyses each test all possible jet-quark assignments and then use alternative criteria to choose the "best" one for each event. The template analysis uses the technique described in [10]: jet energies float within expected resolutions, b-tagged jets are assigned to b quarks, and the top-quark mass is left floating in the fit while the W-boson masses are constrained to 80.4 GeV/c^2. The algorithm described in [14, 11, 12] is used in the convolution analysis. The jet-quark assignment is selected using constraints on the W-boson mass, the $t\bar{t}$ mass difference, the transverse energy in the reconstructed $t\bar{t}$ pair with respect to the total transverse energy in the event, and the b-jet probability of the jets. Although the algorithms to reconstruct the kinematics of the $t\bar{t}$ pairs are different, the $\cos\theta^*$ resolution for each analysis is estimated to be the same (≈ 0.35) from studies using generated $t\bar{t}$ events.

In both analyses the W-boson helicity fractions are determined from maximum likelihood fits to the resulting $\cos\theta^*$ distributions. The two analyses employ alternative methods to derive the fit inputs which will be discussed in more detail in the next paragraphs. In the fits, the helicity fractions f_0 and f_+ are free parameters, the constraint $f_- = (1 - f_0 - f_+)$ is applied, and the background contribution is allowed to float but is Gaussian constrained using an RMS corresponding to the uncertainty on the estimate of the total number of background events. As already discussed in sec. 1, each analysis performs three different measurements. In two measurements we determine f_0 or f_+ and

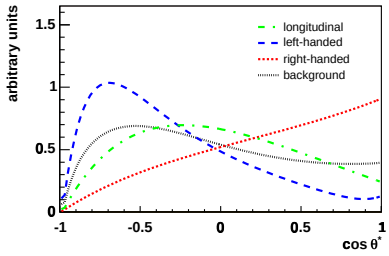

Figure 1: The $\mathcal{P}(\cos\theta^*)$ used in the template analysis, which are the reconstructed $\omega(\theta^*)$ distributions for longitudinal, right- and left-handed W-boson helicities, as well as the $\omega(\theta^*)$ in the background model. The curves are normalized to the same area.

fix the other parameter to the value expected in case of a pure $V-A$ structure of the Wtb vertex ($f_0 = 0.7$, $f_+ = 0.0$). In the third measurement, f_0 and f_+ are both treated as free parameters and are measured simultaneously.

The template method utilizes samples of generated $t\bar{t}$ events in which the leptonically decaying W boson is forced to a specific polarization to get the normalized $\cos\theta^*$ probability distribution function $\mathcal{P}(\cos\theta^*)$ for each W-boson polarization. These generated events satisfy all the selection criteria and are reconstructed in the same manner as the observed events. The $\mathcal{P}(\cos\theta^*)$ for a certain helicity mode is obtained by fitting the reconstructed $\cos\theta^*$ distribution obtained from the corresponding generated $t\bar{t}$ events and does not depend on the helicity fractions assumed for the hadronically decaying W boson. The background modeling is verified by comparing the distribution obtained from generated events to the distribution of observed events in which there is no secondary vertex tag and in those for which the decay length of the secondary vertex tag is negative, meaning that the reconstructed secondary vertex and the reconstructed jet itself are located in opposite hemispheres with respect to the primary vertex. These are background dominated samples. The $\mathcal{P}(\cos\theta^*)$ parameterizations are empirically chosen to provide a good description of the $\cos\theta^*$ distributions and use a third degree polynomial times two exponential functions. The resulting $\mathcal{P}(\cos\theta^*)$ are compared in Fig. 1. Using alternative fit functions, negligibly affects the results.

Since the kinematics of the W-boson decay depend on its polarization, the kinematic cuts applied have different acceptances for the different polarizations and alter the observed composition of polarization states. The largest impact is due to the isolation requirement and the cut on the p_T of the charged lepton. Therefore a correction is applied to the obtained helicity fractions to account for these acceptance effects before presenting the results.

In the convolution analysis the $\cos\theta^*$ distribution is reconstructed in six bins, corresponding to the resolution of the reconstruction of the $t\bar{t}$ kinematics. The starting point for the extraction of the W-boson helicity fractions in this method is the theoretically predicted number of signal events in each bin of

source	δf_0		δf_+		δf_0		δf_+	
	f_+ fixed		f_0 fixed		combined fit		combined fit	
	templ.	conv.	templ.	conv.	templ.	conv.	templ.	conv.
JES	0.024	0.045	0.017	0.025	0.021	0.016	0.027	0.032
ISR	0.002	0.010	0.003	0.003	0.010	0.036	0.007	0.014
FSR	0.021	0.025	0.009	0.011	0.025	0.045	0.002	0.016
Bkg	0.023	0.032	0.016	0.019	0.018	0.028	0.017	0.032
MC	0.019	0.012	0.009	0.005	0.019	0.015	0.010	0.002
PDF	0.005	0.005	0.005	0.002	0.005	0.014	0.002	0.006
Total	0.044	0.062	0.027	0.034	0.043	0.072	0.034	0.050

Table 2: The sources of systematic uncertainties and their related estimates for the template analysis (templ.) and the convolution analysis (conv.). The total systematic uncertainty is taken as the quadrature sum of the individual sources.

the $\cos\theta^*$ distribution, $\mu^{\rm sig}(f_0, f_+)$, depending on f_0 and f_+, which can be calculated using Eq. 2. Acceptance and resolution effects are then taken into account [14] by convoluting both effects with the theory prediction. This leads to the number of signal events expected to be observed in a certain bin accounting for all distorting effects:

$$\mu_k^{\rm sig,obs}(f_0, f_+) \propto \sum_i \mu_i^{\rm sig}(f_0, f_+) \cdot \epsilon_i \cdot S(i,k). \tag{4}$$

The migration matrix element $S(i,k)$ gives the probability for an event which was generated in bin i to occur in bin k of the reconstructed $\cos\theta^*$ distribution. Since the acceptance depends on $\cos\theta^*$, we weight the contribution of each bin with its event selection efficiency ϵ_i. The effects considered are independent of the W-boson helicity fractions and this is validated using several samples of generated events with different W-boson polarizations. Thus, ϵ_i and $S(i,k)$ can be estimated from a sample of events generated with the PYTHIA event generator using the standard settings. The total number of events expected to be observed in a certain bin is then given by the sum of $\mu_k^{\rm sig,obs}(f_0, f_+)$ and the expected number of background events, which is independent of the W-boson polarization and is derived from the background composition shown in Table 1. In a maximum-likelihood fit the expected number of events is compared bin by bin to the number of observed events to determine f_0 and f_+.

In order to compare our observations with theory, we subtract the background estimate from the reconstructed $\cos\theta^*$ distribution, correct for acceptance and resolution, and normalize the distribution to the $t\bar{t}$ cross section of $\sigma_{t\bar{t}} = 6.7 \pm 0.9$ pb [25, 26]. The correction is made by applying a bin-by-bin correction factor to the $\cos\theta^*$ distribution. The correction factor is given by $\mu_i^{\rm sig}(f_0^{\rm fit}, f_+^{\rm fit})$ divided by $\mu_i^{\rm sig,obs}(f_0^{\rm fit}, f_+^{\rm fit})$, where $f_0^{\rm fit}$ and $f_+^{\rm fit}$ are the obtained results.

The systematic uncertainties associated with the measurement of f_0 and f_+

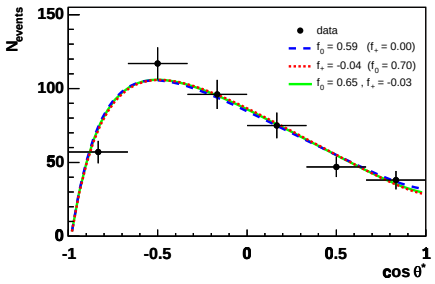

Figure 2: The observed $\cos\theta^*$ distribution (points) overlaid with the fit-curves for the three different fit-scenarios (as explained in sec. 1) for the template analysis.

are summarized in Table 2. The systematic uncertainties were determined by constructing ensemble tests with signal and/or background templates, affected by the systematic under study, but fit using the default parameterizations and normalizations described above. We studied the influence of variations in the jet energy scale (JES), of initial and final state radiation (ISR, FSR), of the background modeling (Bkg), of different Monte Carlo event generators (MC), and of the parton distribution function (PDF). The resulting shifts in the mean fitted longitudinal and right-handed fraction are used to quantify the systematic uncertainties. The positive and negative variations obtained are symmetrized by choosing the maximum deviation. The ensemble tests were all performed using PYTHIA generated events with $m_t = 175$ GeV/c^2 as signal with the W-boson helicity fractions $f_0 = 0.70$ and $f_+ = 0.0$, and the background model as described above. We have verified that these uncertainties do not depend on the actual value of f_0 and f_+ by fitting samples of generated events with different W-boson polarizations. The analyses presented in this paper use a top-quark mass of 175 GeV/c^2. Since f_0 explicitly depends on the top-quark mass, the dependency of the measured value of f_0 on the top quark mass is not treated as a systematic uncertainty. The measured value of f_+ is only negligibly affected by variations in the assumed top-quark mass.

6. Results and Combination of the Results

The $\cos\theta^*$ distribution from the observed events is shown in Fig. 2 and Fig. 3 for both analyses together with the fits for f_0 and f_+ and the model independent measurement. The results for the three different measurements together with the statistical and systematical uncertainties in both analyses are summarized in Table 3. In the template analysis the correlation between f_0 and f_+ is determined to be -0.87 in the simultaneous fit, while for the convolution analysis the correlation is -0.89.

We combine the single results accounting for correlations using the BLUE method [27]. The combined results can be found in Table 3. The statistical cor-

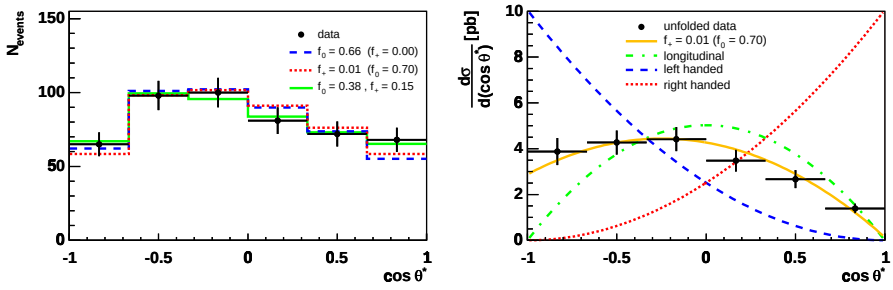

Figure 3: On the left-hand side the observed $\cos\theta^*$ distribution (points) is presented overlaid with the fits for f_0 and f_+ for the convolution analysis. On the right-hand side the deconvoluted (using the fit result of the f_+ measurement) distribution normalized to the $t\bar{t}$ cross-section is shown together with the theoretically predicted curves for purely left-handed, right-handed, and longitudinally polarized W bosons.

relation between both analyses is estimated from ensemble tests using samples of generated events which account for the event overlap in the signal contribution. For the two model-dependent scenarios the correlation coefficients are found to be 0.66 and 0.65 when fitting for f_0 or f_+, respectively. The correlation matrix for the model-independent scenario is given in Table 4.

The systematic uncertainties are taken to be completely correlated between the two methods. When combining the model-independent results the systematic uncertainties for f_0 and f_+ are taken to be 100% anti-correlated. The combined values of f_0 and f_+ have a correlation of -0.82. The combination improves the sensitivity by about 10% relative to the measurements of either method separately.

In conclusion, we present two different analyses and their combination determining the W-boson helicity fractions in top-quark decays, giving the world's most sensitive result for measuring these fractions so far. In addition to measuring f_0 and f_+ separately, while fixing the other parameter to its expected value, we present a model-independent simultaneous measurement of the two fractions. All of these results are consistent with the values predicted within

	template	convolution	combination	χ^2/dof
$f_0(f_+ = 0.0)$	$0.59 \pm 0.11 \pm 0.04$	$0.66 \pm 0.10 \pm 0.06$	$0.62 \pm 0.10 \pm 0.05$	$0.7/1$
$f_+(f_0 = 0.7)$	$-0.04 \pm 0.04 \pm 0.03$	$0.01 \pm 0.05 \pm 0.03$	$-0.04 \pm 0.04 \pm 0.03$	$1.8/1$
f_0	$0.65 \pm 0.19 \pm 0.04$	$0.38 \pm 0.21 \pm 0.07$	$0.66 \pm 0.16 \pm 0.05$	$4.3/2$
f_+	$-0.03 \pm 0.07 \pm 0.03$	$0.15 \pm 0.10 \pm 0.05$	$-0.03 \pm 0.06 \pm 0.03$	$4.3/2$

Table 3: Results of the template analysis, the convolution analysis, and the combined values. The results are given together with their statistical and systematical uncertainties. In addition the χ^2/dof of the combination is given.

	template f_0	convolution f_0	template f_+	convolution f_+
template f_0	1.00	0.45	-0.87	-0.40
convolution f_0	0.45	1.00	-0.42	-0.89
template f_+	-0.87	-0.42	1.00	0.48
convolution f_+	-0.40	-0.89	0.48	1.00

Table 4: Correlation matrix for combining the template and convolution analyses in the model-independet scenario.

the electroweak theory of the Wtb vertex.

Acknowledgements

We thank the Fermilab staff and the technical staffs of the participating institutions for their vital contributions. This work was supported by the U.S. Department of Energy and National Science Foundation; the Italian Istituto Nazionale di Fisica Nucleare; the Ministry of Education, Culture, Sports, Science and Technology of Japan; the Natural Sciences and Engineering Research Council of Canada; the National Science Council of the Republic of China; the Swiss National Science Foundation; the A.P. Sloan Foundation; the Bundesministerium für Bildung und Forschung, Germany; the Korean Science and Engineering Foundation and the Korean Research Foundation; the Science and Technology Facilities Council and the Royal Society, UK; the Institut National de Physique Nucleaire et Physique des Particules/CNRS; the Russian Foundation for Basic Research; the Ministerio de Ciencia e Innovación, and Programa Consolider-Ingenio 2010, Spain; the Slovak R&D Agency; and the Academy of Finland.

References

[1] T.D. Lee and C.N. Yang, Phys. Rev. 105, 1671 (1957). Nucl. Phys. 3, 127 (1957). A. Salam, Nuov. Cim. 5, 299 (1957). R.P. Feynman and M. Gell-Mann, Phys. Rev. 109, 193 (1958). E.C.G. Sudarshan and R.E. Marshak, Phys. Rev. 109, 1860 (1958).

[2] Tevatron Electroweak Working Group, "A Combination of CDF and DØ Results on the Mass of the Top Quark", arXiv:0808.1089 [hep-ex].

[3] R.D. Peccei and X. Zhang, Nucl. Phys. B 337, 269 (1990).

[4] W. M. Yao *et al.* (Particle Data Group), J. Phys. G 33 (2006) 1.

[5] G.L Kane, G.A. Ladinski and C.P. Yuan, Phys. Rev. D 45, 124 (1992).

[6] C.-R. Chen, F. Larios, and C.-P. Yuan, Phys. Lett. B 631, 126 (2005); arXiv:hep-ph/0503040v3 (2008).

[7] M. Fischer *et al.*, Phys. Rev. D 63, 031501(R) (2001).

[8] M. Jezabek and J.H. Kühn, Nucl. Phys. B 314, 1 (1989); Phys. Lett. B 207, 91 (1988). A. Czarnecki and K. Melnikov, Nucl. Phys. B 544, 520 (1999). K.G. Chetyrkin, R. Harlander, T. Seidensticker, and M. Steinhauser, Phys. Rev. D 60, 114015 (1999).

[9] M. Fischer, S. Groote, J.G. Körner, and M.C. Mauser, Phys. Rev. D 63, 031501(R) (2001). H.S. Do, S. Groote, J.G. Körner, and M.C. Mauser, Phys. Rev. D 67, 091501(R) (2003).

[10] A. Abulencia *et al.*, (CDF Collaboration), Phys. Rev. D 73, 032003 (2006).

[11] D. Hirschbuehl, Ph.D. thesis, University of Karlsruhe, FERMILAB-THESIS-2005-80 (2005).

[12] Th. Chwalek, Diplom thesis, University of Karlsruhe, FERMILAB-MASTERS-2006-04 (2006).

[13] T. Aaltonen *et al.*, (CDF Collaboration), submitted to Phys. Rev. Lett., arXiv:0806.2472v2 [hep-ex].

[14] A. Abulencia *et al.* (CDF Collaboration), Phys. Rev. D 75, 052001 (2007).

[15] V. M. Abazov *et al.* (DØ Collaboration), Phys. Rev. Lett. 100, 062004 (2008).

[16] D. Acosta *et al.* (CDF Collaboration), Phys. Rev. D 71, 031101(R) (2005).

[17] A. Bhatti *et al.* (CDF Collaboration), Nucl. Instrum. Methods A566, 375(2006).

[18] A. Abulencia *et al.* (CDF Collaboration), Phys. Rev. Lett. 97, 082004 (2006).

[19] T. Sjostrand, P. Eden, C. Friberg, L. Lonnblad, G. Miu, S. Mrenna and E. Norrbin, Comput. Phys. Commun. 135, 238 (2001).

[20] G. Corcella, I.G. Knowles, G. Marchesini, S. Moretti, K. Odagiri, P. Richardson, M.H. Seymour and B.R. Webber, hep-ph/0011363, hep-ph/0210213.

[21] M.L. Mangano *et al.*, J. High Energy Phys. 0307, 001 (2003).

[22] J. Alwall *et al.*, J. High Energy Phys. 0709, 028 (2007).

[23] T. Affolder *et al.*, Nucl. Instrum. Methods A447, 1(2000).

[24] S. Moed, Ph.D. thesis, University of Geneva, FERMILAB-THESIS-2007-70 (2007).

[25] N. Kidonakis and R. Vogt, Phys. Rev. D 68, 114014 (2003).

[26] M. Cacciari *et al.*, J. High Energy Phys. 0404, 068 (2004).

[27] L. Lyons, D. Gibaut, P. Clifford, Nucl. Inst. Meth. A270 (1988); A. Valassi, Nucl. Inst. Meth. A500 (2003).